Forecast Informed Reservoir Operations within a Satellite Based Framework for Mountainous and High Precipitation Regions: The case of the 2018 Kerala floods

Pritam Das[1], Sarath Suresh[2], Faisal Hossain[3], Vivek Balakrishnan[4], Jainet P J[5], Hyongki Lee[6], Miguel Laverde[7], Kamal Hosen[8], Chinaporn Meechaiya[9], Peeranan Towashiraporn[10]

[1]Graduate Student, Department of Civil and Environmental Engineering, University of Washington, Seattle, WA, USA; email: pdas47@uw.edu

[2]Graduate Student, Department of Civil and Environmental Engineering, University of Washington, Seattle, WA, USA; email: saraths@uw.edu

[3]Professor, Department of Civil and Environmental Engineering, University of Washington, Seattle, WA, USA; email: fhossain@uw.edu (Corresponding author)

[4]Scientist, KSCSTE-Centre for Water Resources Development and Management, Kerala, India; email: vivek@cwrdm.org

[5]Scientist, KSCSTE-Centre for Water Resources Development and Management, Kerala, India; email: jainet@cwrdm.org

[6]Professor, Department of Civil and Environmental Engineering, University of Houston, Houstain, TX, USA; email: hlee45@central.uh.edu

[7]Researcher, Asian Disaster Preparedness Center, Bangkok, 10400, Thailand; email: miguel.laverde@adpc.net

[8]Researcher, Asian Disaster Preparedness Center, Bangkok, 10400, Thailand; email: kamal.hosen@adpc.net

[9]Researcher, Asian Disaster Preparedness Center, Bangkok, 10400, Thailand; email: chinaporn.m@adpc.net

[10]Researcher, Asian Disaster Preparedness Center, Bangkok, 10400, Thailand; email: peeranan@adpc.net

ABSTRACT:

River regulation in mountainous and high precipitation regions with hydropower dams often struggles to find the right balance between hydropower generation while ensuring flood protection for downstream inhabitants. The goal of hydropower generation is to keep reservoirs at the maximum pool as often as possible while for flood control, it is to maintain sufficient cushion in available storage to absorb an incoming flood wave. Using weather forecasts to proactively manage reservoir operations for such conflicting goals is now a well-known solution. However, this challenge of applying forecast-informed reservoir operations is magnified in developing regions where there is a paucity of ground data to track reservoir dynamics. In this study, we explore the utility of using publicly available precipitation forecast from the Global Ensemble Forecasting System (GEFS) with a fully satellite-based reservoir tracking framework called Reservoir Assessment Tool (RAT) to understand the potential of forecast-informed operations in highly mountainous and high precipitation regions that are mostly ungauged. We apply our investigation to the case of damaging floods that took place in 2018 in the Southern Indian state of Kerala where river regulation is carried out with a fleet of hydropower dams. Our results show that the precipitation forecast from GEFS has sufficient skill, if focused on trends and bias adjustment, to predict reservoir inflow peaks up to a week ahead of time where the trend for timing of the peak and rate of rise match well. Using our satellite-based RAT framework, we explore the range of actionable scenarios for dam operators that could potentially minimize downstream flood risk with this forecast-informed reservoir operations scheme.

KEYWORDS: Mountainous basins, precipitation, flood control, satellite remote sensing, forecasting, reservoir operations, and Kerala.

1. Introduction

Floods affect millions of people resulting in loss of life, livelihoods, and damage to infrastructure each year. An estimated 23% of the world population is directly exposed to catastrophic floods, among which about 90% live in low- to middle-income countries, with limited ability to cope with such disasters (Rentschler et al. 2022). Such floods, especially in mountainous regions with steep slopes can be made more disastrous by extreme precipitation events, such as the devastating floods and landslides in Uttarakhand, India, in 2013; in Kerala, India in 2018, and in South Korea in 2023 (Shah 2023; Shin 2023; Vijaykumar et al. 2021). An increase in the intensity and frequency of such extreme precipitation events has been observed globally, especially in the past decade (Dunn et al. 2020; Sun et al. 2021). Climate models suggest that such extreme precipitation events are very likely to keep increasing in frequency and intensity due to climate change making such floods more frequent (Fischer et al. 2015; Intergovernmental Panel on Climate Change 2014; Kharin et al. 2018; Li et al. 2021).

Reservoirs play a crucial role in providing a cushion against such floods. However, they are often optimized for multiple purposes, such as flood control and hydropower, for maximizing the benefits of existing infrastructure (Ahmad and Hossain 2020). Due to the competing nature of optimization strategies of such reservoirs, floods that are exacerbated due to extreme precipitation events in mountainous regions pose additional risks for reservoir operations. For instance, hydropower dams in Kerala (India) in 2018 were faced with floods due to extreme precipitation, which were almost full for hydropower generation (Vijaykumar et al. 2021). This led to little-to-no storage cushioning to mitigate the impending flood pulse, leading to full-scale devastation of the unattenuated flood pulse downstream. Consequently, the flood event claimed the lives of over 489 people, displaced over 1.4 million people, and caused damages of more than $5 billion (Pramanick et al. 2022; Suresh et al. 2024).

During such extreme flood events, forecasted information about the impending flood could be potentially useful in informing reservoir operators to be proactive. Recent forensic studies on the Kerala 2018 floods present a dichotomy of views. Mishra et al. (2018) report that a week's lead time in forecasting could have potentially mitigated the situation with proactive reservoir operations. On the other hand, a study by Sudheer et al. (2019) claims that no amount of forecasting could have helped given how anomalous and extreme the precipitation patterns were during that time. Regardless of the debate, the value of such forecasted information arguably depends on the flexibility in the operation of reservoirs afforded to the reservoir operators, because reservoirs are operated on predefined rule curves mixed with the dam operator's situational awareness of the evolving situation. However, there is no doubt that if the peak of the catastrophic flood wave was forecasted sufficiently ahead of time and in an actionable manner, dam operators could have acted on the forecasted information early. For example, with a sufficient lead time, forecasted incoming flood can be potentially mitigated of its risk posed by reducing the peak flow rate downstream through early release to make room for flood storage (Saavedra Valeriano et al. 2010).

With longer forecast lead times, the skill of the forecasts gradually degrades (Siqueira et al. 2020). Anghileri et al. (2016) reported that the value of long-term streamflow (seasonal to inter-annual) forecasting has limited value for designing adaptive reservoir operation strategies. Instead, streamflow forecasting and reservoir optimization at a shorter time scales, with lead times of days to a few weeks, is more suited for preparedness against floods (Wang et al. 2012). In addition to flood preparedness, forecasted reservoir inflow can also pave the way for forecast-informed adaptive management for more efficient hydropower production where the dual and conflicting goals of flood control and hydropower can be maintained (Ahmad and Hossain 2020; Anghileri et al. 2016).

Operational streamflow forecasting has been a topic of great interest, and decision support systems exist at varying spatial and temporal scales. For instance, the GloFAS system uses short-term daily meteorological forecasts and long-term climatological data to forecast streamflow globally using the Lisflood hydrological model (Van Der Knijff et al. 2010). This system performs well for medium-large sized river basins, with low basin water storage, but the performance decreases with decreasing drainage area, which is the case for most of the mountainous basins in the Southwestern coast of India such as in Kerala. Wu et al. (2012) developed the Global Flood Monitoring System (GFMS) which forecasts streamflow at a quasi-global scale, between 50°N-50°S up to a 5-day lead time driven by the GEOS-5 forecasted precipitation. While this system is generally able to detect floods with a probability of detection (POD) of 0.7, the performance reduces with the presence of river regulation that is not explicitly accounted for.

By the end of the century, climate model projections estimate that dams may help reduce the exposure to floods for about 12.9%-20.6% of the population (Boulange et al. 2021). In spite of the important role played by reservoirs, they are either not considered by hydrological models or their incorporation in modeling is highly parameterized due to a lack of availability of reservoir operations data (Alcamo et al. 2003; Biemans et al. 2011; Haddeland et al. 2006; Hanasaki et al. 2006, 2018). Using publicly available satellite observations covering nearly the entire Earth, reservoir operations, including inflow, storage change, evaporation and outflow from dams, is now being inferred globally from space (Biswas and Hossain 2022; Kumar et al. 2024; Li et al. 2023).

The Reservoir Assessment Tool (RAT) is one such publicly accessible and globally scalable tool, for both operational monitoring and historical analyses of reservoir operations. RAT leverages observations from multiple satellites to infer reservoir operations (Biswas et al. 2021; Das et al. 2022; Minocha et al. 2023). RAT has been set up operationally over various basins across the world for near-real time reservoir operations tracking, such as the Columbia, Mekong, Tigris-Euphrates, Kerala, and is used as an operational decision support system by stakeholders, such as the Mekong River Commission (MRC) and Columbia River Inter-tribal Fish Commission (CRITFC). Given the debate surrounding the value of precipitation forecasting for proactive reservoir operations for Kerala 2018 floods and our ability to track reservoirs from space, we believe it is now important to put the satellite-based modeling of reservoir state within the context of exploring forecast-informed operations to investigate the issue further.

For this study, using meteorological forecasts, including gauge corrected precipitation forecasts, and historical reservoir storage change, we have augmented RAT with a forecasting module. We assess the value added by the forecasting module of the RAT system in informing reservoir operators of forecasted streamflow and exploring reservoir outflows based on actionable reservoir operation scenarios. Specifically, we investigate the utility of forecasts at different lead times over the mountainous basin of Kerala using the 2018 flood as our case study. Our choice for this region is representative of the vast regions in the tropical and developing world where rivers are regulated by hydropower dams, are flood prone and yet often lack ground measurement or public sharing of reservoir state information. The overarching research question of our study is, *how effective are gauge-adjusted precipitation forecasts in informing reservoir operations in highly mountainous and high precipitating regions?* In this study, we address the following objectives:

- To test the effectiveness of forecasted inflow for flood preparedness in mountainous and high precipitation regions using forecasted precipitation by the Global Ensemble Forecast System calibrated to in-situ gauge observations in the South Indian region of Kerala.
- To explore the range of actionable scenarios for dam operators that could have potentially minimized downstream flood risk of the Kerala 2018 floods with this forecast-informed reservoir operations scheme of RAT.

2. Data and Methods

2.1. Study Area

We conducted the investigation over the Greater Periyar basin of Kerala, India. The Periyar river is the longest river in Kerala. Bounded by the Arabian Sea to the West and the Western Ghats mountains to the East, Kerala’s topography varies from low-lying coastal areas to highly mountainous with steep slopes (Fig. 1). Kerala receives most of the annual precipitation due to southwest monsoonal winds during July-September, receiving more than about 3000 mm precipitation annually. The windward slopes of the Western Ghats receive heavy precipitation leading to a high risk of flooding (Simon and Mohankumar 2004; Thomas and Prasannakumar 2016). The Kerala 2018 flood was one of the worst floods in recent history due to an extremely high precipitation event in the month of August. Between August 1 to August 19, 2018, Idukki received more than 700mm of rainfall, which is about 164% more than the normal amount of rainfall during this period (Central Water Commission 2018).

The Periyar river is regulated by 13 dams, with the Idukki dam being the largest. The investigation concentrates on 6 major dams out of the 13, due to their availability in public global dam databases such as The Global Reservoir and Dam (GRanD) database (Lehner et al., 2011). The water management in the basin, especially for the Idukki dam is made challenging by the fact that the upstream reservoir, the Mullaperiyar dam, is operated by the neighboring state of Tamil Nadu, which is under a separate operating jurisdiction than Kerala’s. This jurisdictional complexity, which is common around the world, is a key justification for a satellite-based framework that provides level-playing, publicly accessible and near real-time state of reservoir for all concerned stakeholder agencies.

2.2. Meteorological forecast datasets

The accuracy of streamflow estimation, especially in monsoon driven regions like Kerala, depends significantly on the accuracy of the precipitation estimates used to drive the hydrological modeling.

Here, we used the recently released Climate Hazards Center InfraRed Precipitation with Stations - Global Ensemble Forecasting System (CHIRPS-GEFS) (Harrison et al. 2022) operational precipitation forecast dataset for streamflow forecasting. It is generated by combining the widely used Climate Hazards InfraRed Precipitation with Stations (CHIRPS) product (Funk et al. 2015) with the Global Ensemble Forecast System (GEFS) v12 (Zhou et al. 2022). The GEFS by itself, is a global numerical weather prediction system which operationally forecasts key atmospheric variables at an hourly temporal resolution for the globe (Zhou et al. 2022). The spatial resolution varies from 0.25° for forecasts up to a 10 days lead time and 0.5° for 11-16 days lead time. Within the state of Kerala, there are three stations used for generating the CHIRPS dataset – Trivandrum, Cochin, and Kozhikode. Although none are within the Periyar basin, the closest station is located 75 kms from the Idukki reservoir. Due to the coastal location of the station, it may not be able to appropriately capture the high intensity rainfall experienced at the upper reaches of the Periyar basin, which underscores the paucity of ground data within the basin and the necessity for more accurate satellite based precipitation estimates. However, such numerical weather predictions based meteorological forecasts can have systemic biases, especially at higher lead times, which can lead to higher uncertainties in streamflow predictions, necessitating post-processing bias correction of the precipitation products (Wood et al. 2004; Yang et al. 2020). Furthermore, the low spatial resolution of the GEFS precipitation forecasts at 0.25-0.5º (~25-50 km) is limited in representing the smaller scale precipitation features that control the rainfall-runoff processes in mountainous basins.

Using a quantile-quantile matching algorithm, the observed historical CHIRPS precipitation dataset is used to remove systemic biases in GEFS precipitation forecast. It is then statistically downscaled to 5km leading to the GEFS-CHIRPS forecast data product (Harrison et al. 2022). The other key meteorological variables for streamflow estimation, such as the minimum and maximum temperature, wind speed and wind direction are derived from the Global Forecasting System (GFS). The core global model of GEFS-CHIRPS, the GFS, is a widely used operational global weather forecast model with a lead time of up to 16 days, producing forecasts at an hourly (for the first 120 hours of forecast) to 3-hourly (for the rest of the duration of forecast) temporal resolution and at a spatial resolution of 0.25°.

2.3. Reservoir operations and streamflow datasets

The hindcast streamflow estimates for all the six reservoirs were first estimated using the RAT 3.0 software package, driven by the Variable Infiltration Capacity (VIC) hydrological model (Liang et al. 1994). The model is forced using the GPM-IMERG run (Huffman et al. 2020; Precipitation Processing System (PPS) 2022) precipitation product, and temperature and wind speed data from NOAA CPC Global Temperatures and NCEP-Reanalysis respectively. The timeliness of the "hindcast" estimates of streamflow are limited by the availability of recorded temperature and wind speed, which are available usually at a lag of 2-3 days. We also "nowcast" the streamflow using GPM-IMERG precipitation, specifically, the IMERG-Late product and forecasted temperature and wind speed from the Global Forecasting System (GFS) when hindcast data is unavailable. Finally, we also "forecast" the incoming streamflow into the reservoir using the CHIRPS-GEFS precipitation forecast and the GFS forecasted meteorology. In-situ streamflow observations were obtained, when available, from the local stakeholder agencies for validation of the streamflow nowcast and forecast.

Earlier, Biswas et al. (2021) used long term satellite observations of reservoir surface areas to infer the likely operation rule curves of the reservoirs. These operation rule curves, relating the storage of the reservoirs for a given month as a fraction of the maximum storage capacity, were used to explore a range of actionable scenarios for dam operators that could have potentially minimized downstream flood risk (described in greater detail in section 3.2).

3. Methodology

3.1. Integration in RAT 3.0 and Forecasting Inflow and Evaporation

The developed forecasting module is designed for integration in the RAT 3.0 software package with minimal changes to the existing code base. The RAT works on the basis of mass balance at the reservoir where inflow, storage change and evaporative losses are modeled or estimated from satellite data to estimate the likely outflow (Fig. 2). Here the outflow is an aggregation of reservoir release longitudinally along the river and lateral diversion via irrigation or water supply canals. For more detailed information on the development and theory behind RAT, the reader should refer to Biswas et al. (2021), Das et al. (2022), and Minocha et al. (2023).

The RAT framework has a total of 14 distinct modular steps that can be run to generate various reservoir operations monitoring datasets (see http://www.ratdosc.io for details). Step 1-3 of RAT 3.0 download and process nowcast meteorological observations by satellites – scaling, aligning and clipping to the region of interest in the process, finally generating forcing inputs for the MetSim (Bennett et al. 2020) meteorological disaggregation model, used in the subsequent steps. The proposed forecasting module replicates these steps in essence, producing the forcing inputs for the MetSim model, but uses forecast meteorological inputs instead of nowcast observations. Using the processed meteorological forecast data, steps 3-8 of RAT 3.0 are run, which uses the MetSim, VIC and the VIC Routing (Lohmann et al. 1996) models to model the streamflow forecast estimates at each reservoir. Step 13 of RAT 3.0 is then used to obtain the forecasted evaporation and the inflow to each reservoir (see Minocha et al., 2023 or https://ratdocs.io). The methodology for obtaining forecasted inflow, evaporation and release under different scenarios is described pictorially in Fig. 2.

The RAT-forecasting module was run for all six dams in the Greater Periyar basin. The VIC model of RAT 3.0 used in this study was calibrated against observed inflow for different basins across Kerala (Suresh et al., 2024). Within the Idukki basin, only the observed inflows to the Idukki reservoir were available. The R^2 and NRMSE (as %) values comparing the observed and nowcast inflows for this reservoir were 0.61 and 40% respectively. While the peak inflow values to the reservoir were underestimated, the trends of the rise and fall of the streamflow rate and the timing of the peak flood were predicted well. The inflow forecasts at different lead times were compared against the satellite-observations based nowcast inflow. This comparison allowed an assessment of skill of forecast against a benchmark of nowcast inflow based on satellite precipitation data. The skill of forecasted inflow was evaluated by calculating the coefficient of determination (R^2) and the Root Mean Squared Error normalized by the range (RMSE-range) at different lead times. The results of this comparison are summarized in Fig. 6.

To further visualize the timing and intensity of the flood peak, the forecasted inflow is also presented as a 2D grid of nowcast and forecast values in Fig. 7 (discussed more in section 4.2). The x-axis represents the date within the forecast horizon, while the y-axis represents the date of generating forecast. For any given date in the forecast horizon, the forecasted inflow at shorter lead times can be read by moving down the y-axis. For each day of forecast generation, the forecasted inflow at “X days ahead” can be read by moving right along the x-axis. A discussion on the inferences provided in greater detail in section 4.2. The skill of forecasted inflow was evaluated by calculating the coefficient of determination (R^2) and the Root Mean Squared Error normalized by the range (RMSE-range) at different lead times. The results of this comparison are summarized in Fig. 6 (discussed in section 4.2).

3.2. Reservoir operations and outflow forecasting

Forecasting reservoir operations, specifically the storage change, is fundamentally challenging because it is influenced heavily by the decisions taken by reservoir operators that one cannot predict or forecast ahead of time. Thus, any forecasting of reservoir state, such as forecast of end storage, water level or outflow, will have to be based on potential dam operating scenarios. These scenarios can be assumed from an inferred operating rule curve assuming the dam operator will likely follow based on an historical response, see Biswas et al. (2021), analogous to a ‘business as usual’ scenario. Alternatively, one can assume various dam operating scenarios in reaction to the impending flood that are each physically plausible. Both options are explored here to shed light on the value of forecast-informed reservoir operations.

The scenarios for exploring actionable reservoir operations to mitigate the flood proactively are elaborated as follows.

1. **Target reservoir water level** - The target water level of the reservoir can be specified by the dam operator to simulate the reservoir state in the forecasting horizon, given the forecast of inflow and evaporation. This can be the maximum permissible water level of a reservoir that the dam operator feels should not be exceeded due to dam safety concerns. It can also be a water level lower than the existing water level that the dam operator wants to attain. Thus, if the target level is forecasted to be greater than the current reservoir level, the incoming flow of water is stored until the target level is reached. The stored water is then released if the target water level is estimated to be less than or equal to the current water level. If the target level is lower than the current reservoir level, then the received inflow is released in a temporally constant manner to attain the desired water level.

2. **Fraction of maximum reservoir storage** - The storage change of the reservoir is estimated by considering a range of predefined fractions of maximum reservoir storage capacity that the dam operator deems permissible. For example, a dam operator may try to be conservative and allow little room for reservoir to change storage quickly by selecting a small fraction of maximum reservoir storage the dam is allowed to operate with. On the other hand, a dam operator may

wish to prioritize flood mitigation and allow a larger range for storage change to operate with, thereby allowing more flexibility in outflow and total storage.

3. **Inferred rule curve** - This is operation rule curve-based dam operation where the rule curve is inferred based on historical observations of reservoir operations for the specific time when the flood took place. As mentioned earlier, this is analogous to 'business as usual' scenario. For example, if a certain dam is known to maintain its storage at a certain level during the first week of August based on historical average using past observations, then that is the likely level the dam operator would try to maintain the level at during the flood event. Using historical observations of the storage of the reservoir as a fraction of the maximum storage of reservoir S_t/S_{max} for any time t, the expected storage change in the forecasting horizon (ΔS_{tN}) is obtained as follows -

$$\Delta S_{tN} = (S_{tN}/S_{max} - S_{t0}/S_{max}) \times S_{max}$$

where, t0 is the date when the forecast was generated and tN is the final date of the forecast. If the rule curve dictates a certain storage change during the forecast horizon, and if the net storage change, defined as the difference of rule curve-based storage change and forecasted inflow, is positive, then the inflow received is stored. If the net storage change is negative, then a constant release is made to meet the necessary storage change.

4. **User defined storage change** - The volume of storage change in the forecasting window can also be directly provided to simulate the reservoir state in the forecast horizon. Here, the dam operator may choose to input any custom storage change value (e.g. 15 million m^3 as an example used in this study) to forecast the other reservoir states (outflow and water level). This way, a dam operator can assess the forecast of the reservoir state, including the water level and outflow based on the expected storage change.

The outflow from the reservoir and the corresponding water surface elevation and area are calculated for all the different storage change scenarios. For example, in the first scenario where a target water level is desired, water is accumulated until the target water level is reached. For each time step in the forecast horizon, if the water level of the reservoir is forecasted to be greater than the target water level, the excess volume of water is released as the outflow (O) and the corresponding storage change is calculated as $\Delta S = O - I - E$. Otherwise, water is stored in the reservoir with no outflow and the storage change is calculated as $\Delta S = I - E$. Here, I is the accumulated inflow, E is the accumulated evaporation and ΔS is the storage change, over the total lead time (T). The change in water elevation is then calculated as ΔH = ΔS/Area. The new water surface elevation of the reservoir is updated using the change in elevation as $H_t = H_{t-1} + \Delta H_t$. The corresponding new surface area is then calculated using the Area-Elevation Curve (AEC). The AEC relates the elevation of the reservoir with the surface area. It can be obtained by surveying the corresponding surface area of a filled reservoir for a given elevation which is usually done before construction of the reservoir. However, in-situ AEC data may not always be available publicly, in which case it can also be obtained using Digital Elevation Models (DEM) (Das et al. 2022). We use AEC derived from the Shuttle Radar Topography Mission (SRTM) DEM in this study.

Similarly, for the other reservoir operation scenarios, the volume of expected storage change during the forecast horizon is first estimated. For instance, in case of the scenario of operating within a pre-defined range of maximum storage change (expressed as a fraction of total storage) or user-defined storage change, the constant outflow rate required within the forecast window is estimated as $O = (I - E - \Delta S)/T$. The water surface elevation and area corresponding to the storage change of the reservoir are then calculated for each time step similar to the methodology described above.

4. Results and Discussions

4.1. Skill of forecast precipitation

Before analyzing the skill and performance of forecasted flow, it is helpful to first analyze how the precipitation input to the RAT framework performs at forecast time scales. This analysis can help explain the ensuing skill and performance in forecasted flow as the skill of flow forecasting cannot exceed that of skill of forecasted precipitation.

In Fig. 4, we show the precipitation forecasts by CHIRPS-GEFS against in-situ gauge recorded precipitation. Overall, the bias in CHIRPS-GEFS precipitation forecast is within -0.50 mm and 1.5 mm, which can be considered negligible. We also compared the IMERG satellite precipitation estimates against the precipitation at an in-situ gauge-based precipitation data product called GSOD (Global

Summary of the Day). This GSOD product is available from the National Climate Data Center (NCDC) via NOAA at: https://www.ncei.noaa.gov/access/metadata/landing-page/bin/iso?id=gov.noaa.ncdc:C00516

The specific GSOD station data were extracted for the period of 2015-2024. The average bias in the GPM-IMERG precipitation product over 10 years was negligible at 0.9 mm. This is not to say that multi-sensor precipitation estimation or GEFS has universally low uncertainty in mountainous basins. Both types of precipitation estimation has endemic challenges that are not picked up well due to the paucity and decreasing density of in-situ precipitation gauges as elevation increases. Interested readers can refer to Pradhan et al. (2022).

We also visually compared the GPM-IMERG in Fig. 5. The precipitation forecasts from CHIRPS-GEFS generally underestimates the intensity of the rainfall when compared to IMERG. The magnitude of the underestimation reduces at shorter lead times, but even at 1 to 3 day lead times, high intensity precipitation is often missed or underrepresented. This underestimation combined with representation of a mountainous terrain in a macroscale gridded model (VIC) is expected to compound the skill of forecasted inflow in the RAT framework for a mountainous and high precipitation region.

Our findings regarding the skill of CHIRPS-GEFS as shown in Fig. 5 is not unexpected given the state of the art of global numerical weather prediction and forecasting of precipitation over highly variable and mountainous terrain. Numerical weather predictions perform well in capturing the small scale orographic effects that are the dominant cause of precipitation in mountainous terrain, especially in

South West India. In such cases, dynamic downscaling techniques are necessary for solving the fine scale microphysics from larger scale numerical weather prediction models for skillful predictions.

4.2. Optimal lead time for forecasting flood timing

The inflow to all the six reservoirs in the Greater Periyar basin were forecasted during the period when the flood peaked. This period was from August 10 to August 25, 2018. Lead times ranging from 1 day to 15 days were explored. During the same time period, the inflow was nowcasted using satellite precipitation data. Fig. 6 compares the forecasted and nowcasted inflow at the Idukki reservoir, where the nowcasted inflow is marked as a black line. The observed inflow is shown as the orange line and forecasted inflows are marked as blue circles, with darker shades representing lower lead times. As the lead time of the forecast decreases, the magnitude of forecasted streamflow matches more closely with the magnitude of nowcast satellite based streamflow estimates from RAT. At a lead time of 1-day to 3-day, both the intensity and timing of the peak flood is well predicted. Compared to the observed streamflow, both the streamflow nowcast and forecast estimates are much lower with a constant bias that could be potentially removed operationally (Fig. 6). The bias discrepancy can be explained by the extreme nature of the precipitation event (Mishra et al. 2018), which can be challenging for both Numerical Weather Prediction models and satellite based observations to detect and estimate the magnitude over mountainous regions (Harrison et al. 2022). Even with the systematic bias between the satellite-based streamflow estimates and observed streamflow, the timing of the flood and the rate of increase in the magnitude of the streamflow during the flood can be seen to be forecasted very well (Fig. 6).

Fig. 7 visually represents the forecasted inflow at different lead times as a 2D grid. Forecasts generated on August 4 to August 12 all indicated a peak in the hydrograph with high streamflow around August 16-17, coinciding with the peak of the actual flood event. Within a lead time of 2-3 days, both the magnitude and timing of the streamflow was forecasted with much certainty. Overall, forecasts with lower lead times of up to 7 days were able to better predict the timing and magnitude of the flood event.

The quantitative performance metrics demonstrating the skill of forecast streamflow at different lead times are shown in Fig. 8. To generate this figure, the inflow forecasts were first generated from July 17 to August 30, 2018, for 15 days beyond each date of generating forecast. For each day within the forecast period, forecasts from different lead times were grouped together. These forecasts, made by varying lead times, were treated as individual time-series. These forecast time series at varying lead times were compared against the nowcast inflow considering it as the baseline for the period when the flood peaked, 15th August to 21st August, 2018.

The R^2 values increase with decreasing lead times. The timing of the peak flood can be quantified at least a week in advance (Fig 8). The metrics denote the performance of forecast during the peak of the flood, from August 15 to August 21, across all the dams in the Greater Periyar basin. High R^2 and low RMSE values of the forecast for all dams a week prior to the peak flood underline the ability of CHIRPS-GEFS precipitation forecast to forecast floods in the mountainous regions.

The somewhat oscillating structure of the R^2 in Fig. 8 can be explained to some extent by the precipitation forecast patterns generated at different lead times. For instance, in Fig 9, we can see that the forecasted precipitation for 15th August generated on 10th August to 12th August suggest that the Idukki basin would receive in excess of 100 mm rainfall, with gradual increase in intensity with decreasing lead time. However, the forecasts generated on August 12 and 14th predict a lower amount of precipitation over the basin as compared to the forecasts on previous days. Such a pattern is expected from Numerical Weather Prediction models as it tries to solve for an ever changing dynamic system that evolves rapidly over the duration of a storm. Hence the change in forecasted precipitation amount over different lead times results in a similar pattern of modeled inflow to the reservoir.

4.3. Exploring actionable reservoir operations based on forecasts and range of scenarios

In this section, we explore the second objective of our study - to explore the range of actionable scenarios for dam operators that could have potentially minimized downstream flood risk of the Kerala 2018 floods with this forecast-informed reservoir operations scheme of RAT. However, before moving into reservoir operation scenarios, let us remind ourselves where the state of the art is in terms of quantitative precipitation forecasting which in turn represents the upper limit of reservoir flow forecasting. For example, the actual outflow from the Idukki reservoir was in the range of 1100-1460 (m3/s) during 15-17 August, 2018 and inflow was in the range of 1440-2000 (m3/s). The actual precipitation on 15th August, 2018 reported by the Indian Meteorological Department (IMD) was in the range of 170-270 mm. Compared to the observed rainfall, the forecasted precipitation over the region was barely above 100mm. The 2018 storm in Kerala was therefore an extreme rainfall event (~200 year return period), an event that the global numerical weather prediction modeling would be limited in capturing its finer physical features without further dynamic downscaling (see section 4.1).

Downstream flood risk is defined as the additional risk posed by uncontrolled release of water from a dam when the incoming volume of water during a flood exceeds that of the flood cushion capacity of the dam. In such cases, downstream inhabitants would experience high inflows at times that do not correspond to the natural timing of a flood if the dam was not there, as common intuition would dictate. This makes such floods even more dangerous due to the unpredictability of the timing of flood for downstream inhabitants, making dissemination of information about dam releases especially important. For this, the reader should refer to the various scenarios defined in section 3.3 that a dam operator is likely to operate the dam by. Outflow scenarios are explored to reduce the flood risk by releasing water at a controlled rate, possibly lower than the rate of flow during the peak flood.

To maintain the water level at a target elevation, water is first withheld or stored until the target level is reached, and then released at a rate equal to the peak inflow flow rate of the flood. This scenario lets users simulate the outflow required to maintain a target water level. For instance, a target water level of 801m was simulated for the Sholayar reservoir, which is 10 m below its full water level (FWL) of 811m for dam safety. In this simulated case, water could be stored until August 19th based on the initial storage of the reservoir on August 10^{th} (2018).

In case of storage change experienced by the reservoirs equaling to ±0.5%, ±2.5% and ±4.0% of the maximum storage capacity, the outflow from the reservoir at a constant rate is selected as a range of possible values deemed safe for downstream inhabitants. In all the simulated scenarios plotted in fig. 10, the rate of outflow is lower than the peak flow rate of the flood entering the reservoir. The high volume of water incoming to the reservoir is compensated by releasing water proactively before the flood peak. The respective reservoir water levels are plotted alongside the corresponding scenarios in Fig. 10 (a and b). This range of forecasted outflows and the corresponding water levels provide a range of possible reservoir operation scenarios for the reservoir operators to consider for minimizing the impact of the flood risk downstream.

The outflow from the dam based on inferred rule curve or historical reservoir operations varies on a case-by-case basis for the reservoirs. This is expected, as each dam and reservoir have unique flood routing and spillway capacity along with a unique bathymetry for storage. It simulates a baseline scenario of the forecast of reservoir states if dam operators operated the reservoirs in a 'business as usual' mode continuing the practice of previous years. For instance, if the Sholayar reservoir was operated according to how it had been operated historically, the water level would be higher by about 3 meters on average compared to the other storage change scenarios. Similarly, the reservoir operator can also simulate the corresponding outflow required and the water level using custom storage change values to simulate the reservoir state based on the expected storage change (Fig. 10).

Based on the different reservoir operation scenarios the forecast of outflow from the reservoirs provide a range of possible forecast-informed reservoir operations scenarios to mitigate or minimize the downstream flood risk. These scenarios can help answer questions such as, (1) how much buffer time can be expected for a target water level to be reached? (2) how would the water level change for different release scenarios given the forecasted inflow? (3) compared to how the reservoirs were operated historically, how would the reservoir state differ based on the release scenarios? (4) could the reservoir operations be adapted to lower the risk posed by the flood?

As discussed in the previous section, the magnitude of the flood was underestimated by both the nowcast and forecasted streamflow but only with a systematic bias that could be removed operationally if needed. Moreover, the timing and the rate of increase in streamflow throughout the week were forecasted very skillfully at a lead time of 7 days (fig. 10). Hence the outflow forecasts in Fig. 10 are representative of the expected outflow for different operation scenarios given the forecasted streamflow, rather than being the "prediction" of the outflow from the reservoirs. Such forecasting of reservation state based solely on satellite observations and publicly available GEFS-CHIRPS data has value for the vast ungauged regions of the world where in-situ data is largely inaccessible.

4.4. Scalability of RAT-Forecasting: the recent August 2024 floods of Tripura and Southeastern Bangladesh

We set up a similar example of forecasting reservoir inflow and scenario-based outflow for the Northeastern region of Tripura (India) and Southeastern Bangladesh, wherein the issue of flood preparedness takes an international angle due to transboundary flow (Fig 11). During August 21-27, 2024, floods that took place first in the upstream region of Tripura (in India) on the Gomti river basin, eventually travelled downstream to Bangladesh. With heavy precipitation, Southeastern Bangladesh was also flooded. The flooding and heavy precipitation in Tripura led to the opening of all gates of the Dumboor dam (India) due to it being at near full reservoir level prior to the flood. Using our RAT framework forced with satellite data and CHIRPS-GEFS, we obtained similar results and inference as we get for the 2018 floods in Kerala (see Fig. 12). Within a 3-day lead time, the intensity and timing of the peak flood is well predicted, and an indication of high inflow is obtained nearly a week prior. Readers can now access the realtime operational system for Tripura/Bangladesh at https://depts.washington.edu/saswe/tripura and for Kerala at https://depts.washington.edu/saswe/kerala.

5. Discussion and Conclusions

Dams and reservoirs play an important role in mitigating risk of flooding for downstream inhabitants. However, reservoir operators often must balance the competing goals of hydropower production and flood control. This is especially challenging in mountainous regions where reservoir operations are optimized for hydropower generation, but also need to address the mitigation of fast response extreme precipitation events. Reservoir operations based on static rule curves, designed based on seasonal inflow patterns often fail to handle rapidly evolving floods driven by climate-change of extreme precipitation events that occur at low exceedance probabilities. As mentioned earlier, the 2018 floods in Kerala, an out-of-season extreme precipitation event left the reservoir operators with limited options for flood mitigation. Hence, it is crucial that such events are forecast, and the forecasts applied to generate guidance for forecast-informed reservoir operations to mitigate potential damages downstream.

In this study, we investigated the ability of a gauge corrected precipitation forecast product, the CHIRPS-GEFS, in forecasting the inflow during the extreme precipitation event of 2018 in Kerala. We explored a range of actionable scenarios for dam operators that could potentially minimize downstream flood risk with this forecast-informed reservoir operations scheme of RAT. For the extreme flood experienced by Kerala in August 2018, the magnitude of the flood peak was not captured with sufficient accuracy. However, the timing of the flood peak and the rate of increasing flow was forecasted quite well with a week's notice using forecasted precipitation from GEFS-CHIRPS. Moreover, the performance in forecasting the timeliness of the flood increased at shorter lead times, although the performance was found to vary from each reservoir. Our exploration of the range of actionable scenarios of reservoir operations based on inflow forecasts within the satellite-based RAT framework revealed that for most cases, the reservoir operator could have made proactive decisions related to reservoir operations to potentially mitigate the flood.

The forecasting module developed for RAT and investigated in this study using the Kerala 2018 floods as a case study (and also for Northeastern region of Tripura, India and Southeastern Bangladesh) demonstrates its promise for application in similar regions and extreme precipitation environments around the world. In that spirit of empowering dam operators and managers of regulated river basins of the world, we have made the forecast module an integral part of the RAT 3.0 software package. Interested readers should visit www.satellitedams.net and https://github.com/UW-SASWE/RAT to access this version of RAT along with its documentation on http://ratdocs.io for implementing RAT 3.0 in forecast mode using GEFS-CHIRPS at a river basin of their interest. Given that RAT is a publicly available, open-source and open-science reservoir tracking software package (Minocha et al. 2023), it is our hope that forecast-informed reservoir operations within a satellite-based tracking framework will improve flood management in regulated river basins where in-situ data or public access to information is scarce.

In closing, the key innovation to the body of knowledge in our opinion is the advancement on the use of weather forecasting for reservoir operations in developing regions of the world that are mountainous with high precipitation (shown in Fig. 13). These are the regions where satellite data are often the only viable alternative (and hence the use of RAT as the reservoir tracking tool; Minocha et al. 2023), as demonstrated through a scalable application in the Indian region of Tripura and Southeastern Bangladesh.

DATA AVAILABILITY STATEMENT:

All the data, except for the in-situ reservoir inflow data to the Idukki dam, used in this study are publicly accessible. Forecast precipitation as the CHIRPS-GEFS dataset was obtained from the Climate Hazards Center at UC Santa Barbara from https://chc.ucsb.edu/data/chirps-gefs. The minimum, maximum temperatures and the U- and V- components of wind are obtained from the historical archives at the Research Data Archive at the National Center for Atmospheric Research (https://rda.ucar.edu/datasets/ds084.1/dataaccess/). The RAT software can be installed using the conda package manager or from https://github.com/UW-SASWE/RAT. Install instructions and the documentation for RAT are available at http://ratdocs.io. The documentation for RAT-Forecasting module and the data associated with this study can also be accessed at https://rat-satellitedams.readthedocs.io/en/latest/Plugins/Forecasting/. The forecasted data generated for the study is available at https://www.dropbox.com/scl/fo/9hbdmu5wbh5wowd95qdsu/ADejOG0KT2FiSnQ8yJKacXk?rlkey=w3z2mk41kasx2ldx5futuifrs&dl=0.

ACKNOWLEDGEMENTS:

This study was supported by NASA Applied Science grants from the Water Resources Program (80NSSC22K0918) and the Capacity Building Program (80NSSC23K0184). All co-authors from the University of Washington and co-author Lee from University of Houston, were supported by both these programs. The Kerala State Electricity Board (KSEB) provided valuable feedback on RAT highlighting the requirements of stakeholders from such a tool which helped improve the overall software package.

REFERENCES:

Ahmad, S. K., and F. Hossain. 2020. “Maximizing energy production from hydropower dams using short-term weather forecasts.” *Renewable Energy*, 146: 1560–1577. https://doi.org/10.1016/j.renene.2019.07.126.

Alcamo, J., P. Döll, T. Henrichs, F. Kaspar, B. Lehner, T. Rösch, and S. Siebert. 2003. “Development and testing of the WaterGAP 2 global model of water use and availability.” *Hydrological Sciences Journal*, 48 (3): 317–337. https://doi.org/10.1623/hysj.48.3.317.45290.

Anghileri, D., N. Voisin, A. Castelletti, F. Pianosi, B. Nijssen, and D. P. Lettenmaier. 2016. “Value of long-term streamflow forecasts to reservoir operations for water supply in snow-dominated river catchments.” *Water Resources Research*, 52 (6): 4209–4225. https://doi.org/10.1002/2015WR017864.

Bennett, A., J. Hamman, and B. Nijssen. 2020. “MetSim: A Python package for estimation and disaggregation of meteorological data.” *JOSS*, 5 (47): 2042. https://doi.org/10.21105/joss.02042.

Biemans, H., I. Haddeland, P. Kabat, F. Ludwig, R. W. A. Hutjes, J. Heinke, W. von Bloh, and D. Gerten. 2011. “Impact of reservoirs on river discharge and irrigation water supply during the 20th century.” *Water Resources Research*, 47 (3). https://doi.org/10.1029/2009WR008929.

Biswas, N. K., and F. Hossain. 2022. “A Multidecadal Analysis of Reservoir Storage Change in Developing Regions.” *Journal of Hydrometeorology*, 23 (1): 71–85. American Meteorological Society. https://doi.org/10.1175/JHM-D-21-0053.1.

Biswas, N. K., F. Hossain, M. Bonnema, H. Lee, and F. Chishtie. 2021. “Towards a global Reservoir Assessment Tool for predicting hydrologic impacts and operating patterns of existing and planned reservoirs.” *Environmental Modelling & Software*, 140: 105043. https://doi.org/10.1016/j.envsoft.2021.105043.

Boulange, J., N. Hanasaki, D. Yamazaki, and Y. Pokhrel. 2021. “Role of dams in reducing global flood exposure under climate change.” *Nat. Commun.*, 12 (1): 417. Nature Publishing Group. https://doi.org/10.1038/s41467-020-20704-0.

Central Water Commission. 2018. *Kerala Floods of August 2018*.

Das, P., F. Hossain, S. Khan, N. K. Biswas, H. Lee, T. Piman, C. Meechaiya, U. Ghimire, and K. Hosen. 2022. “Reservoir Assessment Tool 2.0: Stakeholder driven improvements to satellite remote sensing based reservoir monitoring.” *Environmental Modelling & Software*, 157 (105533). https://doi.org/10.1016/j.envsoft.2022.105533.

Dunn, R. J. H., L. V. Alexander, M. G. Donat, X. Zhang, M. Bador, N. Herold, T. Lippmann, R. Allan, E. Aguilar, A. A. Barry, M. Brunet, J. Caesar, G. Chagnaud, V. Cheng, T. Cinco, I. Durre, R. De Guzman, T. M. Htay, W. M. Wan Ibadullah, M. K. I. Bin Ibrahim, M. Khoshkam, A. Kruger, H. Kubota, T. W. Leng, G. Lim, L. Li-Sha, J. Marengo, S. Mbatha, S. McGree, M. Menne, M. De Los Milagros Skansi, S. Ngwenya, F. Nkrumah, C. Oonariya, J. D. Pabon-Caicedo, G. Panthou, C. Pham, F. Rahimzadeh, A. Ramos, E. Salgado, J. Salinger, Y. Sané, A. Sopaheluwakan, A. Srivastava, Y. Sun, B. Timbal, N. Trachow, B. Trewin, G. Van Der

Schrier, J. Vazquez-Aguirre, R. Vasquez, C. Villarroel, L. Vincent, T. Vischel, R. Vose, and M. N. Bin Hj Yussof. 2020. “Development of an Updated Global Land In Situ-Based Data Set of Temperature and Precipitation Extremes: HadEX3.” *JGR Atmospheres*, 125 (16): e2019JD032263. https://doi.org/10.1029/2019JD032263.

Fischer, A. M., D. E. Keller, M. A. Liniger, J. Rajczak, C. Schär, and C. Appenzeller. 2015. “Projected changes in precipitation intensity and frequency in Switzerland: a multi-model perspective.” *Intl. Journal of Climatology*, 35 (11): 3204–3219. https://doi.org/10.1002/joc.4162.

Funk, C., P. Peterson, M. Landsfeld, D. Pedreros, J. Verdin, S. Shukla, G. Husak, J. Rowland, L. Harrison, A. Hoell, and J. Michaelsen. 2015. “The climate hazards infrared precipitation with stations—a new environmental record for monitoring extremes.” *Sci. Data.*, 2 (1): 150066. https://doi.org/10.1038/sdata.2015.66.

Haddeland, I., T. Skaugen, and D. P. Lettenmaier. 2006. “Anthropogenic impacts on continental surface water fluxes.” *Geophys. Res. Lett.*, 33 (8): L08406. https://doi.org/10.1029/2006GL026047.

Hanasaki, N., S. Kanae, and T. Oki. 2006. “A reservoir operation scheme for global river routing models.” *Journal of Hydrology*, 327 (1–2): 22–41. https://doi.org/10.1016/j.jhydrol.2005.11.011.

Hanasaki, N., S. Yoshikawa, Y. Pokhrel, and S. Kanae. 2018. “A global hydrological simulation to specify the sources of water used by humans.” *Hydrology and Earth System Sciences*, 22 (1): 789–817. https://doi.org/10.5194/hess-22-789-2018.

Harrison, L., M. Landsfeld, G. Husak, F. Davenport, S. Shukla, W. Turner, P. Peterson, and C. Funk. 2022. “Advancing early warning capabilities with CHIRPS-compatible NCEP GEFS precipitation forecasts.” *Sci. Data*, 9 (1): 375. Nature Publishing Group. https://doi.org/10.1038/s41597-022-01468-2.

Huffman, G. J., D. T. Bolvin, D. Braithwaite, K.-L. Hsu, R. J. Joyce, C. Kidd, E. J. Nelkin, S. Sorooshian, E. F. Stocker, J. Tan, D. B. Wolff, and P. Xie. 2020. “Integrated Multi-satellite Retrievals for the Global Precipitation Measurement (GPM) Mission (IMERG).” *Satellite Precipitation Measurement: Volume 1, Advances in Global Change Research*, V. Levizzani, C. Kidd, D. B. Kirschbaum, C. D. Kummerow, K. Nakamura, and F. J. Turk, eds., 343–353. Cham: Springer International Publishing.

Intergovernmental Panel On Climate Change (Ed.). 2014. “Long-term Climate Change: Projections, Commitments and Irreversibility Pages 1029 to 1076.” *Climate Change 2013 – The Physical Science Basis*, 1029–1136. Cambridge University Press.

Shah, D. 2023. “Kedarnath: ‘Survivors took refuge in trees - and died of hunger.’” *BBC*, June 16, 2023.

Kharin, V. V., G. M. Flato, X. Zhang, N. P. Gillett, F. Zwiers, and K. J. Anderson. 2018. “Risks from Climate Extremes Change Differently from 1.5°C to 2.0°C Depending on Rarity.” *Earth’s Future*, 6 (5): 704–715. https://doi.org/10.1002/2018EF000813.

Kumar, S., S. Imen, V. K. Sridharan, A. Gupta, W. McDonald, J. J. Ramirez-Avila, O. I. Abdul-Aziz, R. Talchabhadel, H. Gao, N. W. T. Quinn, W. J. Weiss, T. Poulose, S. S. Palmate, C. M. Lee, and L. Baskaran. 2024. “Perceived barriers and advances in integrating earth observations with water resources modeling." *Remote Sensing Applications: Society and Environment*, 33: 101119. https://doi.org/10.1016/j.rsase.2023.101119.

Lehner, B., Liermann, C. R., Revenga, C., Vörösmarty, C., Fekete, B., Crouzet, P., ... & Robertson, J. C. 2011. "Global reservoir and dam (grand) database. *Technical Documentation, Version*, 1: 1-14.

Li, C., F. Zwiers, X. Zhang, G. Li, Y. Sun, and M. Wehner. 2021. "Changes in Annual Extremes of Daily Temperature and Precipitation in CMIP6 Models." *Journal of Climate*, 34 (9): 3441–3460. https://doi.org/10.1175/JCLI-D-19-1013.1.

Li, Y., G. Zhao, G. H. Allen, and H. Gao. 2023. "Diminishing storage returns of reservoir construction." *Nat. Commun*., 14 (1): 3203. Nature Publishing Group. https://doi.org/10.1038/s41467-023-38843-5.

Liang, X., D. P. Lettenmaier, E. F. Wood, and S. J. Burges. 1994. "A simple hydrologically based model of land surface water and energy fluxes for general circulation models." *J. Geophys. Res.*, 99 (D7): 14415–14428. https://doi.org/10.1029/94JD00483.

Lohmann, D., R. Nolte-Holube, and E. Raschke. 1996. "A large-scale horizontal routing model to be coupled to land surface parametrization schemes." *Tellus A: Dynamic Meteorology and Oceanography,* 48 (5): 708–721. Taylor & Francis. https://doi.org/10.3402/tellusa.v48i5.12200.

Minocha, Sanchit, Faisal Hossain, Pritam Das, Sarath Suresh, Shahzaib Khan, George Darkwah, Hyongki Lee, Stefano Galelli, Konstantinos Andreadis, and Perry Oddo. Forthcoming. "Reservoir Assessment Tool

Version 3.0: A Scalable and User-Friendly Software Platform to Mobilize the Global Water Management Community." *Geoscientific Model Development Discussions* (2023): 1-23.

Mishra, V., S. Aaadhar, H. Shah, R. Kumar, D. R. Pattanaik, and A. D. Tiwari. 2018. "The Kerala flood of 2018: combined impact of extreme rainfall and reservoir storage." *Hydrology and Earth System Sciences Discussions*, 1–13. https://doi.org/10.5194/hess-2018-480.

Pradhan, R.K., Y. Markonis, Mijael Rodrigo Vargas Godoy, Anahí Villalba-Pradas, Konstantinos M. Andreadis, Efthymios I. Nikolopoulos, Simon Michael Papalexiou, Akif Rahim, Francisco J. Tapiador, Martin Hanel. 2022. "Review of GPM IMERG performance: A global perspective," *Remote Sensing of Environment*, 268, 112754, https://doi.org/10.1016/j.rse.2021.112754.

Pramanick, N., R. Acharyya, S. Mukherjee, S. Mukherjee, I. Pal, D. Mitra, and A. Mukhopadhyay. 2022. "SAR based flood risk analysis: A case study Kerala flood 2018." *Advances in Space Research, Advances in Spaceborne SAR Remote Sensing for Characterization of Natural and Manmade Features - Part 1*, 69 (4): 1915–1929. https://doi.org/10.1016/j.asr.2021.07.003.

Precipitation Processing System (PPS). 2022. "Version 7 Late 24-Hour IMERG_GIS." National Aeronautics and Space Administration.

Rentschler, J., M. Salhab, and B. A. Jafino. 2022. "Flood exposure and poverty in 188 countries." *Nat. Commun.*, 13 (1): 3527. Nature Publishing Group. https://doi.org/10.1038/s41467-022-30727-4.

Saavedra Valeriano, O. C., T. Koike, K. Yang, T. Graf, X. Li, L. Wang, and X. Han. 2010. “Decision support for dam release during floods using a distributed biosphere hydrological model driven by quantitative precipitation forecasts.” *Water Resources Research*, 46 (10). https://doi.org/10.1029/2010WR009502.

Shin, H. 2023. “South Korea flood death toll rises to 40, Yoon blames botched responses.” *Reuters*, July 17, 2023.

Simon, A., and K. Mohankumar. 2004. “Spatial variability and rainfall characteristics of Kerala.” *J. Earth Syst. Sci.*, 113 (2): 211–221. https://doi.org/10.1007/BF02709788.

Siqueira, V. A., F. M. Fan, R. C. D. D. Paiva, M.-H. Ramos, and W. Collischonn. 2020. “Potential skill of continental-scale, medium-range ensemble streamflow forecasts for flood prediction in South America.” *Journal of Hydrology*, 590: 125430. https://doi.org/10.1016/j.jhydrol.2020.125430.

Sudheer, K. P., S. Murty Bhallamudi, B. Narasimhan, J. Thomas, V. M. Bindhu, V. Vema, and C. Kurian. 2019. “Role of Dams on the Floods of August 2018 in Periyar River Basin, Kerala.” *Current Science*, 116 (5): 780. https://doi.org/10.18520/cs/v116/i5/780-794.

Sun, Q., X. Zhang, F. Zwiers, S. Westra, and L. V. Alexander. 2021. “A Global, Continental, and Regional Analysis of Changes in Extreme Precipitation.” *Journal of Climate*, 34 (1): 243–258. https://doi.org/10.1175/JCLI-D-19-0892.1.

Suresh, S., F. Hossain, S. Minocha, P. Das, S. Khan, H. Lee, K. Andreadis, and P. Oddo. 2024. Forthcoming. "Satellite-based Tracking of Reservoir Operations for Flood Management during the 2018 Extreme Weather Event in Kerala, India." *Remote Sensing of Environment*.

Thomas, J., and V. Prasannakumar. 2016. "Temporal analysis of rainfall (1871–2012) and drought characteristics over a tropical monsoon-dominated State (Kerala) of India." *Journal of Hydrology*, 534: 266–280. https://doi.org/10.1016/j.jhydrol.2016.01.013.

Van Der Knijff, J. M., J. Younis, and A. P. J. De Roo. 2010. "LISFLOOD: a GIS-based distributed model for river basin scale water balance and flood simulation." *International Journal of Geographical Information Science*, 24 (2): 189–212. https://doi.org/10.1080/13658810802549154.

Vijaykumar, P., S. Abhilash, A. V. Sreenath, U. N. Athira, K. Mohanakumar, B. E. Mapes, B. Chakrapani, A. K. Sahai, T. N. Niyas, and O. P. Sreejith. 2021. "Kerala floods in consecutive years - Its association with mesoscale cloudburst and structural changes in monsoon clouds over the west coast of India." *Weather and Climate Extremes*, 33: 100339. https://doi.org/10.1016/j.wace.2021.100339.

Wang, F., L. Wang, H. Zhou, O. C. Saavedra Valeriano, T. Koike, and W. Li. 2012. "Ensemble hydrological prediction-based real-time optimization of a multiobjective reservoir during flood season in a semiarid basin with global numerical weather predictions." *Water Resources Research*, 48 (7). https://doi.org/10.1029/2011WR011366.

Wood, A. W., L. R. Leung, V. Sridhar, and D. P. Lettenmaier. 2004. “Hydrologic Implications of Dynamical and Statistical Approaches to Downscaling Climate Model Outputs.” *Climatic Change*, 62 (1): 189–216. https://doi.org/10.1023/B:CLIM.0000013685.99609.9e.

Wu, H., R. F. Adler, Y. Hong, Y. Tian, and F. Policelli. 2012. “Evaluation of Global Flood Detection Using Satellite-Based Rainfall and a Hydrologic Model.” *Journal of Hydrometeorology*, 13 (4): 1268–1284. American Meteorological Society. https://doi.org/10.1175/JHM-D-11-087.1.

Yang, C., H. Yuan, and X. Su. 2020. “Bias correction of ensemble precipitation forecasts in the improvement of summer streamflow prediction skill.” *Journal of Hydrology*, 588: 124955. https://doi.org/10.1016/j.jhydrol.2020.124955.

Zhou, X., Y. Zhu, D. Hou, B. Fu, W. Li, H. Guan, E. Sinsky, W. Kolczynski, X. Xue, Y. Luo, J. Peng, B. Yang, V. Tallapragada, and P. Pegion. 2022. “The Development of the NCEP Global Ensemble Forecast System Version 12.” *Weather and Forecasting*, 37 (6): 1069–1084. https://doi.org/10.1175/WAF-D-21-0112.1.

FIGURE CAPTION LIST:

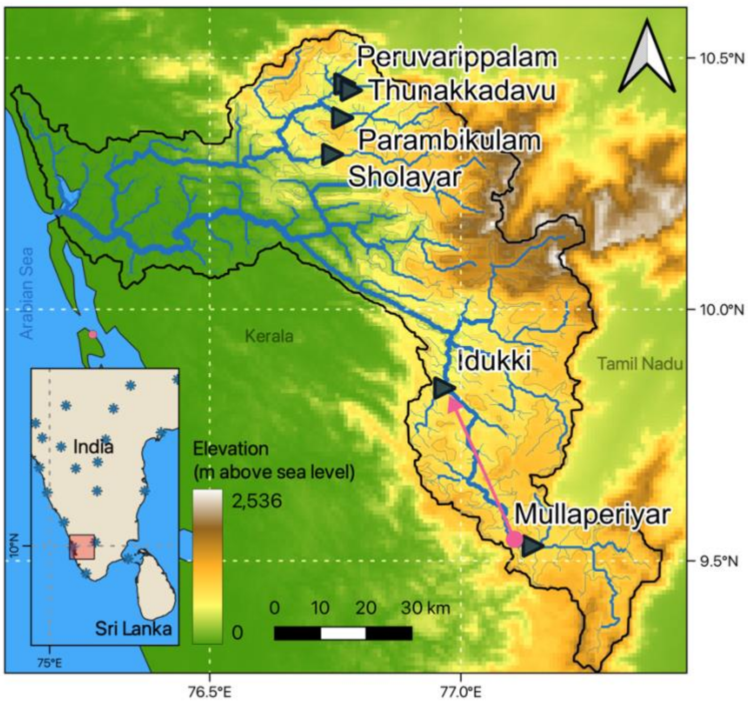

Fig. 1. Map of the Greater Periyar River Basin showing the location of six study reservoirs. A pink arrow highlights the flow of water from the Mullaperiyar Dam to the Idukki Dam. An inset map to the bottom left shows the location of the Greater Periyar basin in the Indian subcontinent, including the location of precipitation measuring stations used in generation of the GEFS-CHIRPS dataset as blue stars.

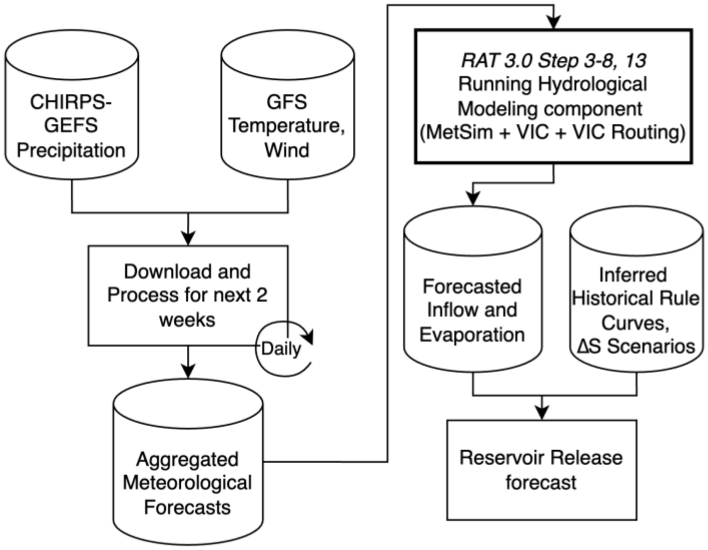

Fig. 2. Flow chart illustrating the methodology for generation of inflow and reservoir outflow forecast.

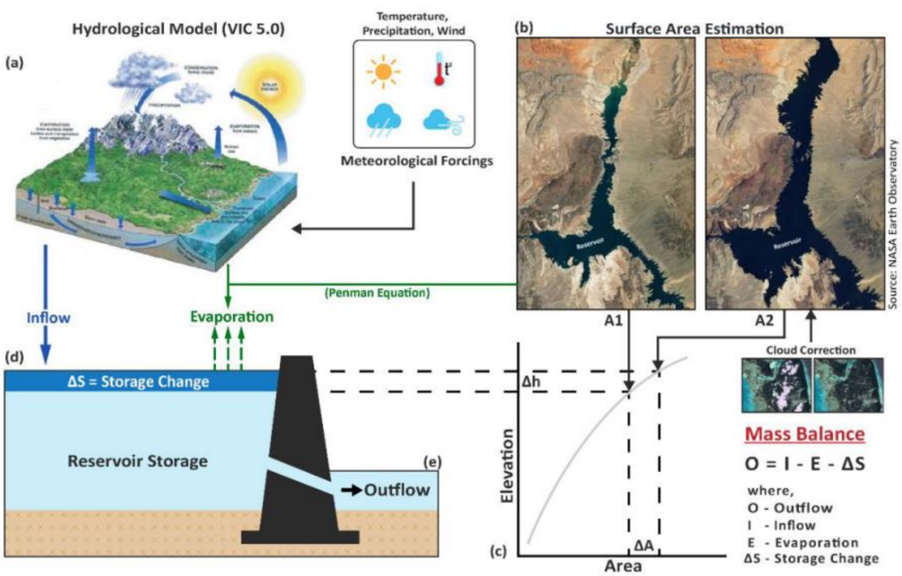

Fig. 3. Illustration of the conceptual model of RAT 3.0. (a) The Variable Infiltration Capacity (VIC) 5.0 hydrological model is used to model the inflow to the reservoir using satellite observations derived meteorological forcings; (b) Surface area is estimated using the TMS-OS algorithm at a frequency of 1-5 days using observations from multiple satellites – Sentinel-1, Sentinel-2 A/B, Landsat 8 and Landsat 9; (c)

Storage change is estimated using observed reservoir surface area and the Area-Elevation relationship of the reservoir; (d) Evaporation is computed using the Penman equation; (e) Using mass balance, outflow is estimation for the reservoirs.

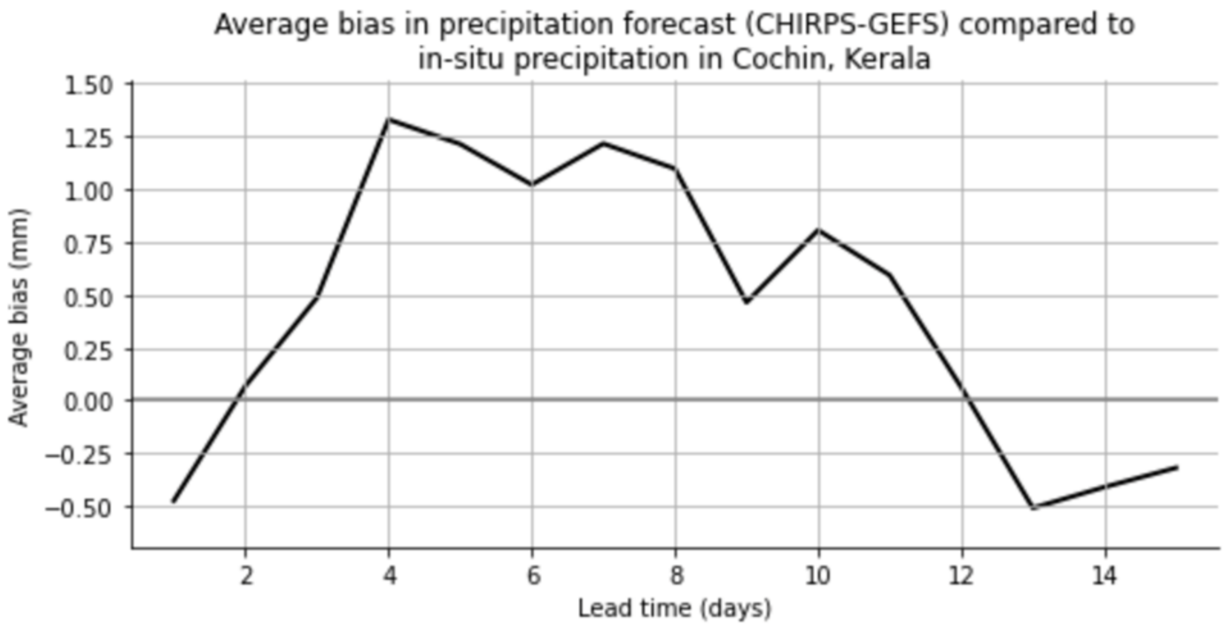

Fig. 4. Comparison of bias, averaged over 2017-2018 CHIRPS-GEFS precipitation forecast at Cochin, Kerala, compared to in-situ gauge measured precipitation.

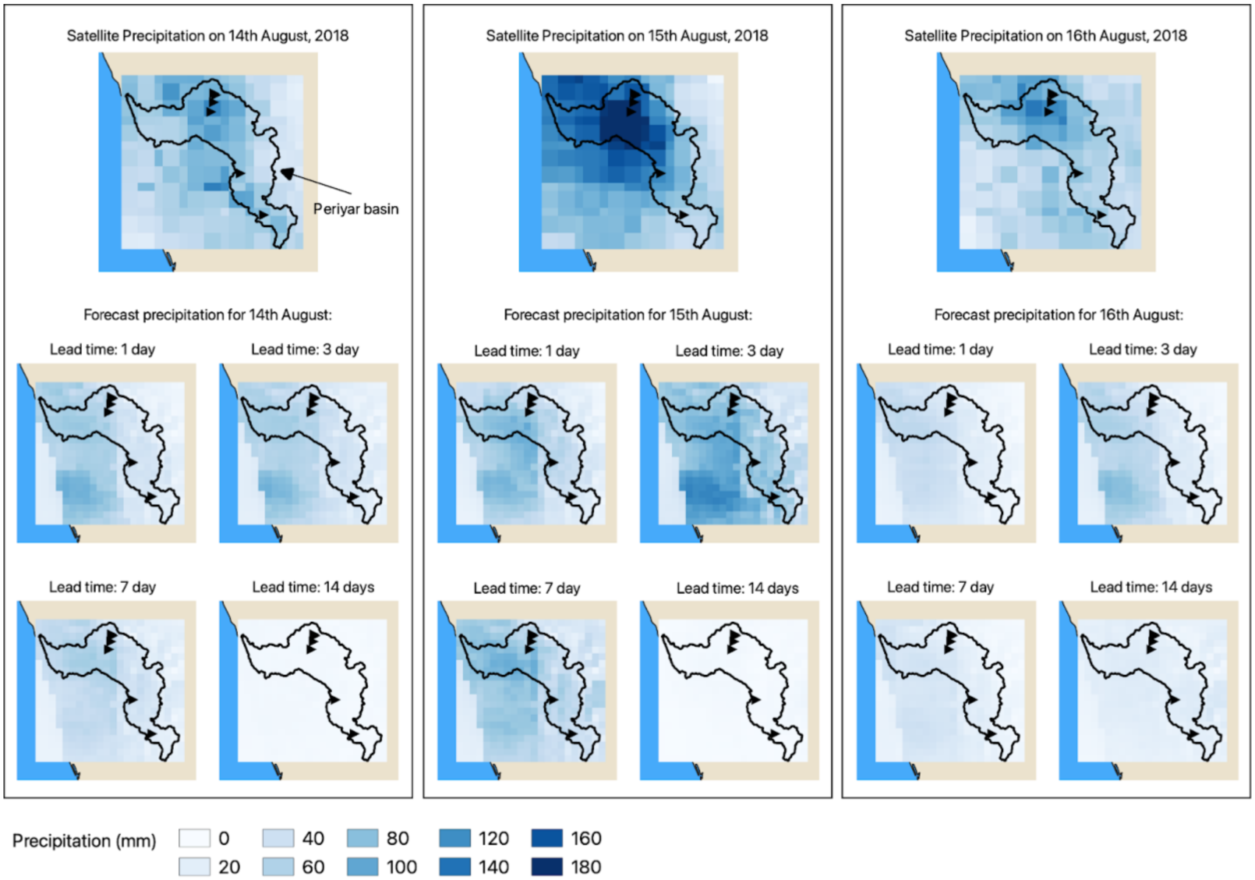

Fig 5: Comparison between IMERG satellite precipitation data (which is nowcast) on the three most intense days of rainfall (14, 15 and 16th August, 2018) and precipitation forecasts for the same days by CHIRPS-GEFS at various lead times. This comparison reveals the potential skill of CHIRPS-GEFS forecast precipitation at various lead times as satellite precipitation is a nowcast (or hindcast) product.

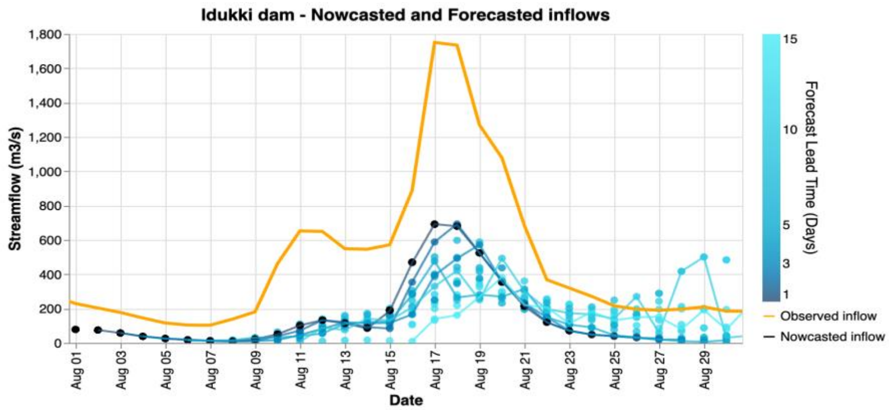

Fig. 6. Comparison of observed inflow (Orange) with inflow modeled using satellite precipitation data using RAT to the Idukki dam (Black line) overlain with forecasted inflow (Blue circles and lines) during the flood in August 2018. Forecasts for lead times 1, 3, 5, 10 and 15 days are highlighted by joining the blue circles representing the forecast time-series.

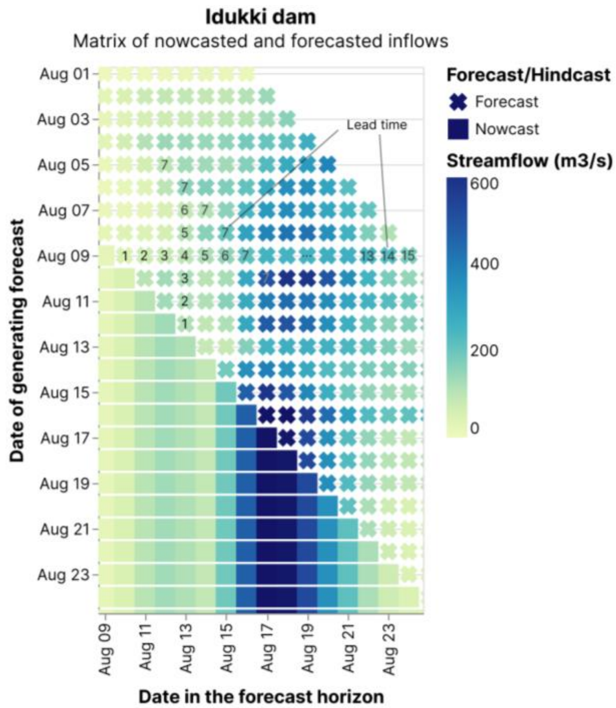

Fig. 7. Matrix of nowcast (squares) and forecast (crosses) streamflow during the peak of the 2018 flood at the Idukki dam. The y-axis represents the date on which the forecast was generated, and the x-axis represents the date of nowcast/forecast. The lead time of forecast increases moving upwards along the y-axis and rightwards on the x-axis. The lead times associated with the forecasted streamflow generated on August 9^{th,} are annotated along the x-axis, and the forecasted streamflow estimated for August 13th are annotated along the y-axis using numbers. The flood peak of August 17th and 18th can be seen to be forecasted with a lead time of about 7-8 days.

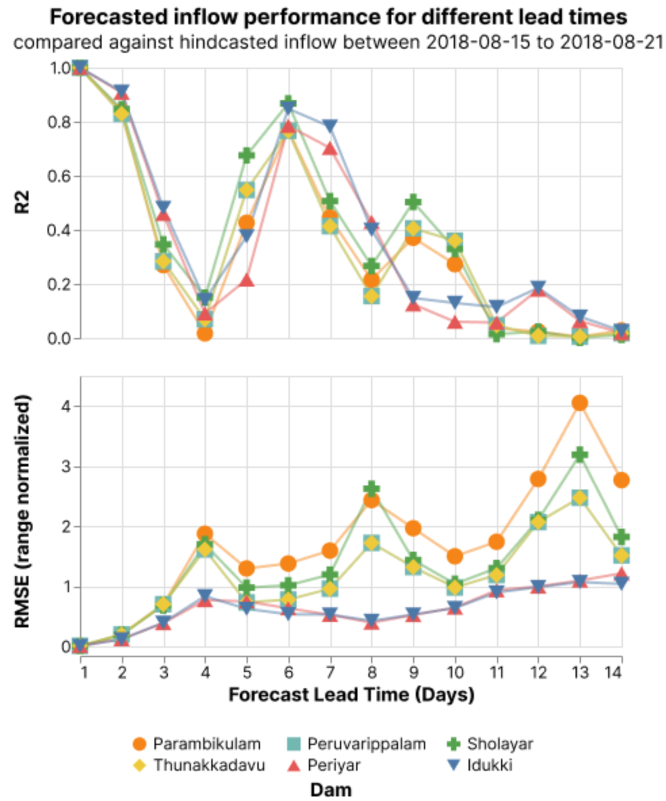

Fig. 8. Performance metrics, R^2 and RMSE (range normalized), comparing the forecasted streamflow estimates at various lead times against nowcasted streamflow during the peak of the flood, between 15th-21st August 2018.

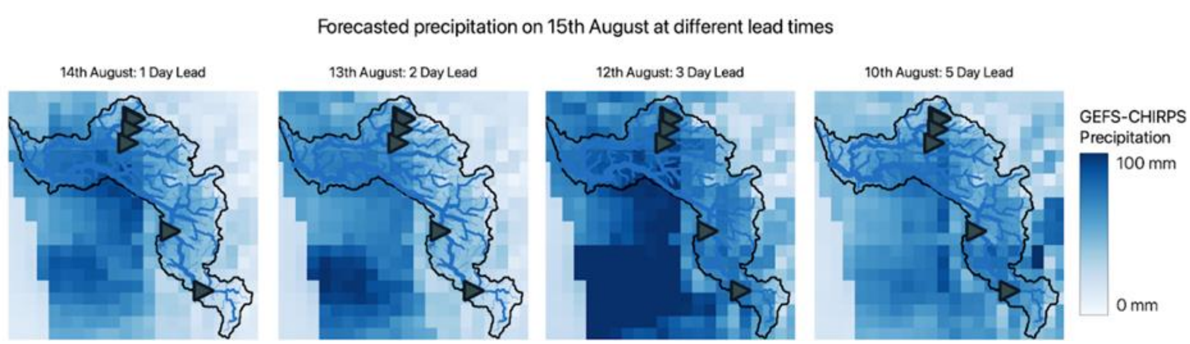

Fig 9. Precipitation forecast of 15th August generated at 1, 2, 3, and 5 day lead times.

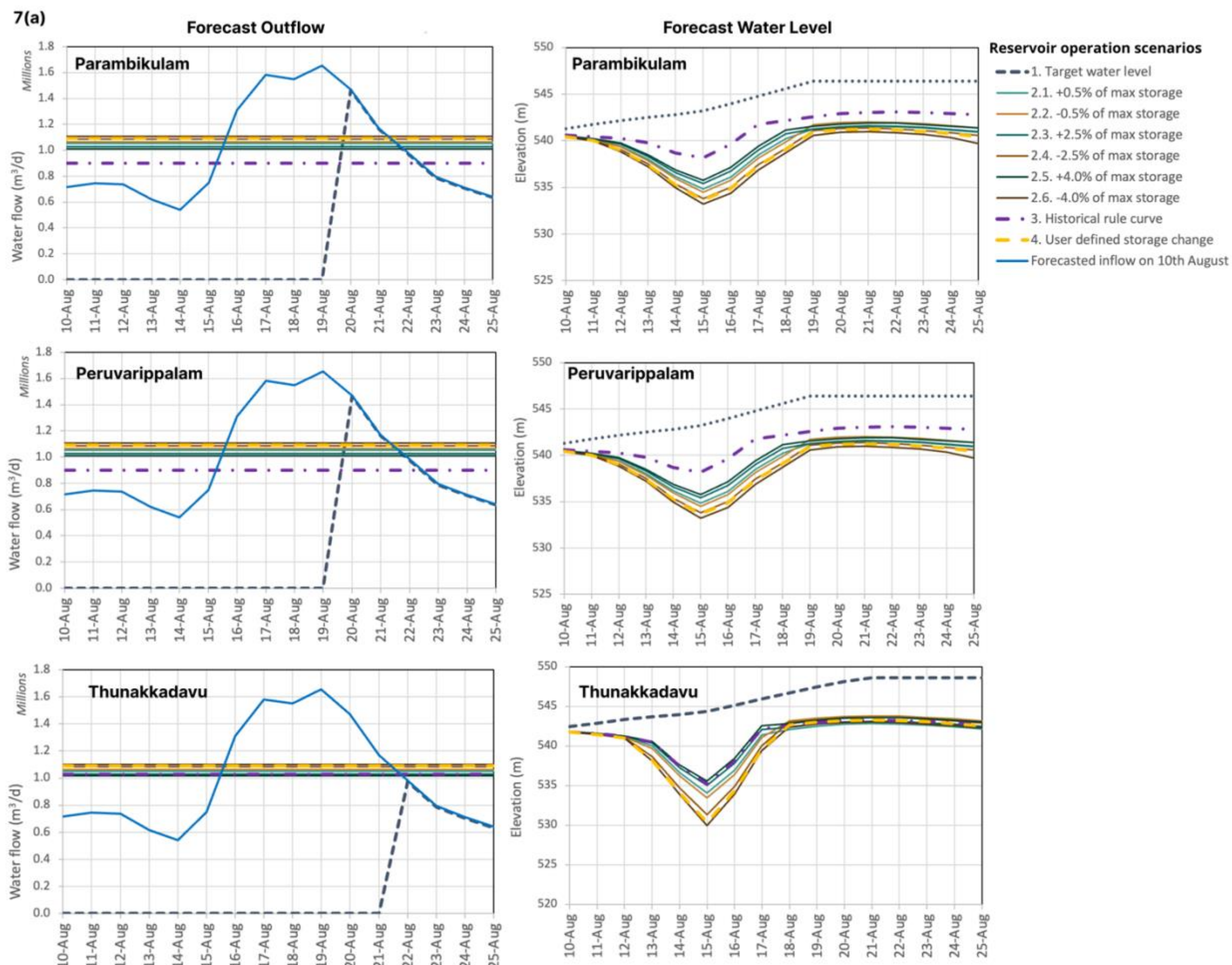

Fig. 10a. Forecasted outflow rates based on different scenarios and their respective forecasted water levels shown for Parambikulam, Peruvarippalam, and Thunakkadavu. Here the blue line on the left panel shows the forecasted inflow generated on day August 10. The idea here is to show how the various dam operator scenarios can potentially mitigate the forecasted inflow (assuming it retained the necessary skill as already seen with up to a 7 day lead time) and attenuate the flood wave with a lower magnitude and more controlled outflow for downstream inhabitants. For dam operating scenarios refer to section 3.2.

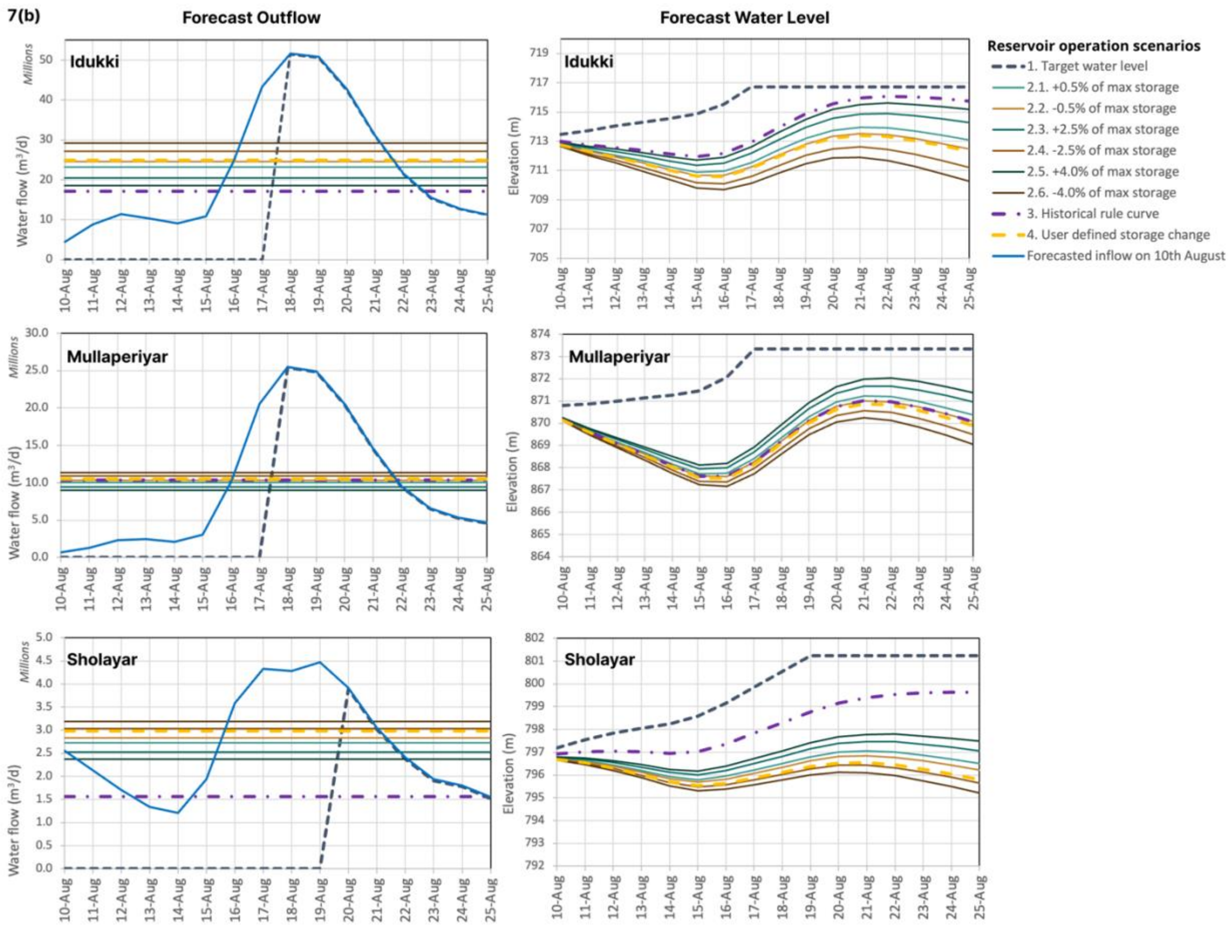

Fig. 10b. Same as Figure 7a but for reservoirs Idukki, Mullaperiyar and Sholayar.

743 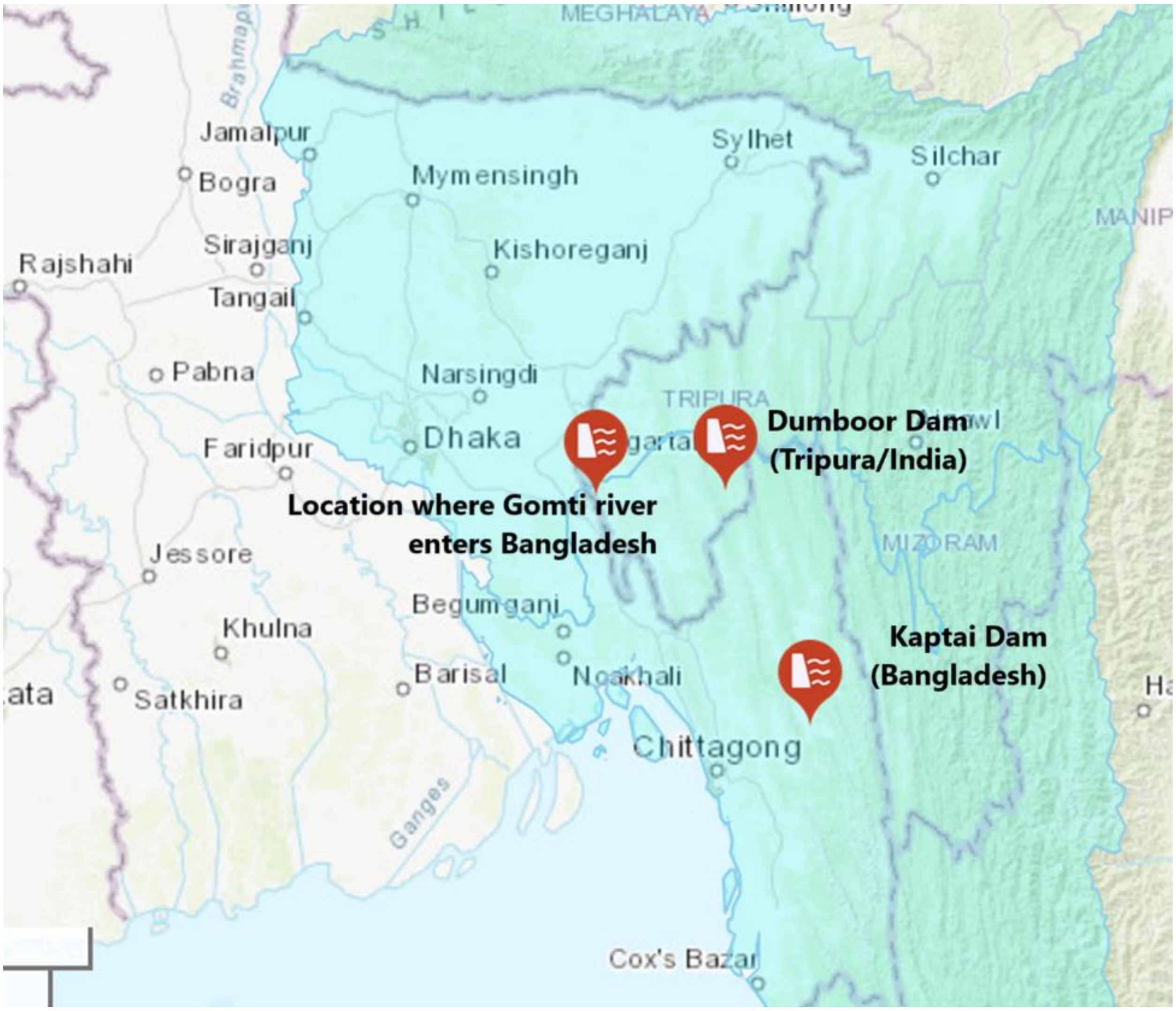

744 **Fig. 11.** Scalability of RAT framework with a recent application in Northeastern state of Tripura and

745 Southeastern Bangladesh to address reservoir operations and transboundary flood preparedness.

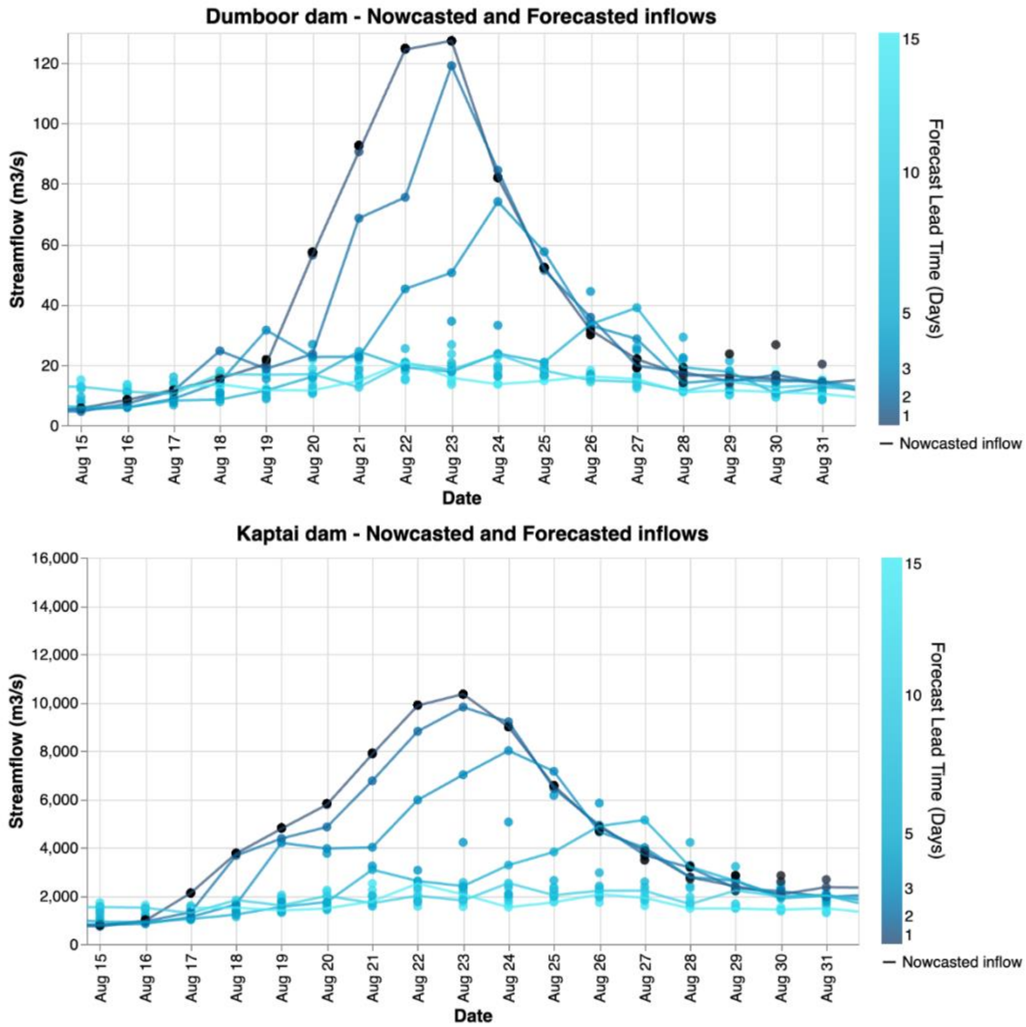

Fig. 12 Inflow forecast to the Dumboor (Tripura, India) and Kaptai (Chittagong, Bangladesh) dams at various lead times (See previous figure for location of dams).

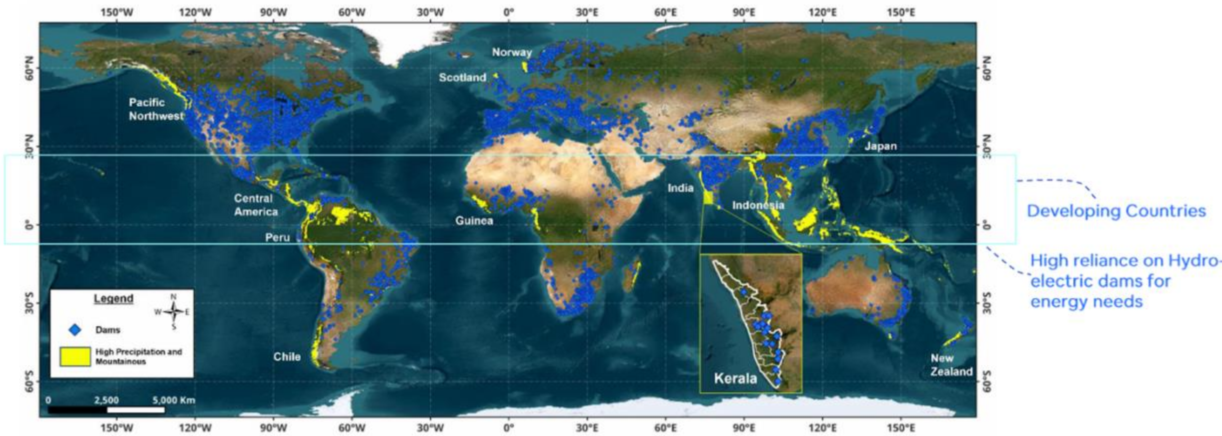

Fig 13. Map showing high precipitation and mountainous regions around the world where this study will be applicable.